

Discontinuous change of shear modulus for frictional jammed granular materials

Michio Otsuki^{1,*} and Hisao Hayakawa²

¹*Department of Physics and Materials Science, Shimane University,
1060 Nishikawatsu-cho, Matsue 690-8504, Japan*

²*Yukawa Institute for Theoretical Physics, Kyoto University,
Kitashirakawaoiwake-cho, Sakyo-ku, Kyoto 606-8502, Japan*

(Dated: March 10, 2022)

The shear modulus of jammed frictional granular materials with the harmonic repulsive interaction under an oscillatory shear is numerically investigated. It is confirmed that the storage modulus, the real part of the shear modulus, for frictional grains with sufficiently small strain amplitude γ_0 discontinuously emerges at the jamming transition point. The storage modulus for small γ_0 differs from that of frictionless grains even in the zero friction limit, while they are almost identical with each other for sufficiently large γ_0 , where the transition becomes continuous. The stress-strain curve exhibits a hysteresis loop even for a small strain, which connects a linear region for sufficiently small strain to another linear region for larger strain. We propose a new scaling law to interpolate between the states of small and large γ_0 .

PACS numbers: 45.70.-n, 05.70.Jk, 81.40.Jj

Introduction.— When the packing fraction ϕ exceeds a critical value ϕ_c , amorphous materials consisting of repulsive particles such as granular materials, colloidal suspensions, foams, and emulsions turn into jammed solids which have rigidity. Such a transition, known as the jamming transition, has been the subject of extensive studies over the last two decades [1, 2]. For frictionless grains, the pressure increases continuously from ϕ_c , while the coordination number Z exhibits a discontinuous transition at ϕ_c in the hard core limit [3, 4].

An assembly of frictionless grains under a simple shear exhibits a rheological continuous transition: the viscosity diverges as ϕ approaches ϕ_c below, while the yield stress increases continuously above ϕ_c [5–27]. The jamming transition is also characterized by the appearance of rigidity under an oscillatory strain above ϕ_c . For sufficiently small strain, the elastic modulus of frictionless grains is independent of the strain and the critical exponents for the jamming transition depend on the type of the local interaction [3, 4, 28]. We call this regime the linear response regime. For large strain, recent studies [29–34] have revealed that the real part of the shear modulus, the storage modulus G , of frictionless particles decreases with increasing strain as a result of nonlinear response because of slip avalanches [35, 36]. The present authors have proposed a scaling law of G to interpolate between the linear and the nonlinear responses [30]. Note that the storage modulus as the ratio of the stress to the strain can be used even in the nonlinear response regime.

Most of previous studies, however, assume that grains are frictionless, though it is impossible to remove contact friction in experiments of dry granular particles and the friction causes drastic changes in rheology such as a discontinuous shear-thickening with a hysteresis loop near

ϕ_c [37–52]. Somfai et al. [53] have numerically investigated the elastic moduli of a frictional system with the aid of the density of state, and found that G/B with the bulk modulus B in the linear response regime is proportional to ΔZ , the excess coordination number relative to the isostatic value. They have also found that ΔZ discontinuously appears at ϕ_c for frictional grains [53]. This suggests that frictional grains with the harmonic repulsive interaction exhibit a discontinuous change of G at ϕ_c even in the frictionless limit contrast to a continuous change for frictionless grains [3, 4, 28].

The difference of the linear elasticity between the frictionless limit and the frictionless case casts doubt on the expectation that the scaling laws for the elasticity of frictionless grains can be confirmed in experiments of grains with sufficiently small friction coefficient. The accessible shear strain in the experiment [29], however, is too large, and does not correspond to the previous theoretical studies [3, 4, 30]. Also, little is known on the nonlinear elasticity of jammed frictional grains. To clarify the effects of the contact friction on the linear and the nonlinear elasticities, we numerically investigate the shear modulus of two-dimensional frictional granular materials near the jamming point under an oscillatory shear.

Setup of Simulation.— Let us consider a two-dimensional assembly of N frictional granular particles. They interact according to the Cundall-Strack model with an identical mass density ρ in a square periodic box of linear size L [54]. The normal repulsive interaction force $F^{(n)}$ is given by $F^{(n)} = k^{(n)}r$ with the compression length r and the normal spring constant $k^{(n)}$, while the tangential contact force $F^{(t)}$ in quasi-static motion is constrained by the Coulomb criterion $|F^{(t)}| \leq \mu F^{(n)}$: $F^{(t)} = k^{(t)}\delta^{(t)}$ in the “stick region” for $|\delta^{(t)}| < \mu F^{(n)}/k^{(t)}$ with the tangential spring constant $k^{(t)}$ and the tangential displacement $\delta^{(t)}$, while $|F^{(t)}|$ remains $\mu F^{(n)}$ in the “slip region” for $|\delta^{(t)}| \geq \mu F^{(n)}/k^{(t)}$. To avoid crystallization, we use a bi-disperse system which includes equal

*otsuki@riko.shimane-u.ac.jp

number of grains of the diameters d_0 and $d_0/1.4$, respectively. The system is subjected to an oscillatory shear with the shear strain $\gamma(t) = \gamma_0 \{1 - \cos(\omega t)\}$, where γ_0 and ω are the strain amplitude and the angular frequency, respectively. Then, we measure the storage modulus defined by [55]

$$G(\gamma_0, \mu, \phi) = -\frac{\omega}{\pi} \int_0^{2\pi/\omega} dt \sigma(t) \cos(\omega t) / \gamma_0, \quad (1)$$

where $\sigma(t)$ is the shear stress. Note that the loss modulus exhibits only a linear dependence on ω and its ϕ -dependence is relatively small [56]. We also point out that G is almost independent of ω when the time period of the oscillatory shear is sufficiently larger than the relaxation time of the configuration of the grains. We, thus, focus on the dependence of G only on γ_0 , μ , and ϕ for sufficiently small ω . Further details of our model and the ω -dependence of the storage and the loss moduli are shown in Ref. [56].

Storage modulus for a given packing fraction.— To begin with, we study the dependence of the storage modulus on the friction coefficient μ . In Fig. 1, we plot G against γ_0 for various μ at $\phi = 0.87$. For each μ , G is almost independent of γ_0 in the linear response regime, while G decreases with γ_0 in the nonlinear response regime. In the linear response regime, G for $\mu > 0$ is almost independent of μ , but differs from that for $\mu = 0$ [53]. In the nonlinear response regime, the storage moduli for $\mu = 0$ and $\mu > 0$ are almost identical with each other. It is noteworthy that the range of the linear response becomes narrower as μ decreases, and G for $\mu = 10^{-5}$ and 10^{-4} have second plateaus. We confirm that storage moduli for various ϕ depend on the order of the limits:

$$\lim_{\mu \rightarrow +0} \lim_{\gamma_0 \rightarrow +0} G(\gamma_0, \mu, \phi) \neq \lim_{\gamma_0 \rightarrow +0} G(\gamma_0, \mu = 0, \phi). \quad (2)$$

The dependence of G on μ and γ_0 in Fig. 1 can be explained from the stress-strain curves shown in Fig. 2, where we plot the intrinsic shear stress $\sigma(\gamma) - \sigma(0)$ against the shear strain γ for various μ at $\gamma_0 = 10^{-6}$ and $\phi = 0.87$. For each μ , $\sigma(\gamma) - \sigma(0)$ is proportional to γ for sufficiently small γ . The proportionality constant for $\mu > 0$ is independent of μ , but is larger than that for $\mu = 0$, which means Eq. (2). The range of the linear response becomes narrower as μ decreases, and the stress-strain curve at $\mu = 10^{-6}$ exhibits a hysteresis loop which connects the first linear region for sufficiently small γ with the second linear region. The gradient for the second linear region is identical to that of the frictionless grains, which results in the second plateau shown in Fig. 1. This behavior has its origin in the change of the tangential friction $F^{(t)}$ from the “stick region” to the “slip region”. See Ref. [56] for the γ_0 -dependence of the stress-strain curve.

Scaling law.— Next, we examine how the storage modulus depends on ϕ . In Fig. 3, we plot G against ϕ for various γ_0 at $\mu = 0.01$. For the smallest strain amplitude ($\gamma_0 = 10^{-6}$), G exhibits a discontinuous transition

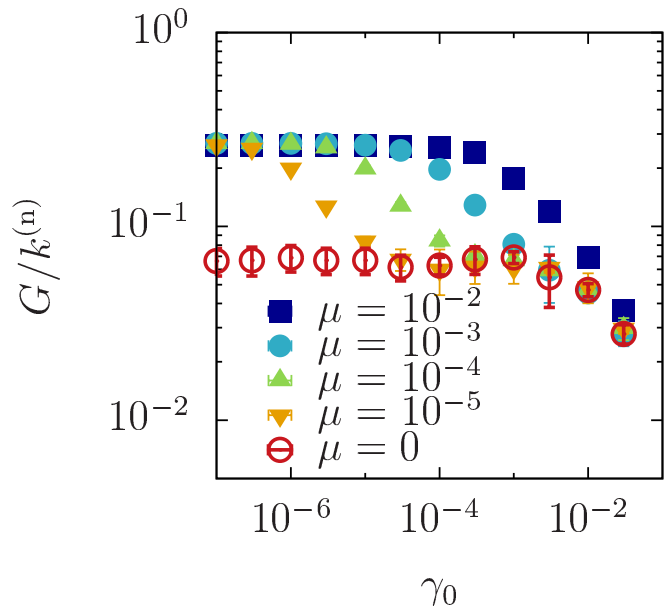


FIG. 1: (Color online) The storage modulus G against γ_0 for $\mu = 10^{-2}$, 10^{-3} , 10^{-4} , 10^{-5} , and 0 at $\phi = 0.87$.

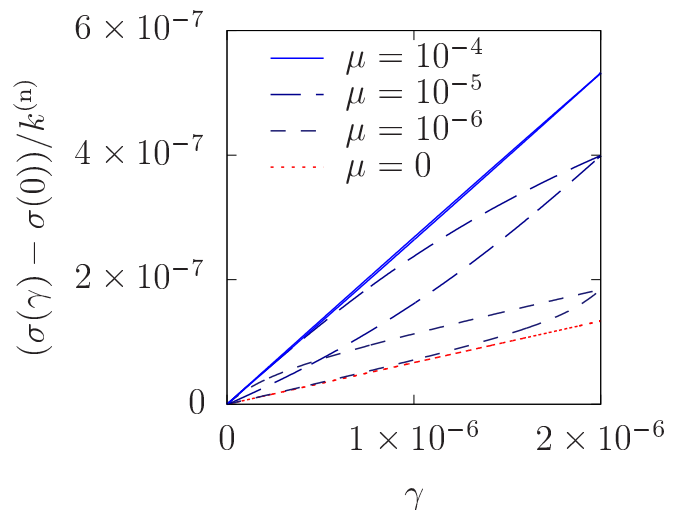


FIG. 2: (Color online) The intrinsic shear stress $\sigma(\gamma) - \sigma(0)$ against γ with $\mu = 10^{-4}$, 10^{-5} , 10^{-6} , and 0 for $\gamma_0 = 10^{-6}$ and $\phi = 0.87$.

at $\phi_c \simeq 0.84$. As γ_0 increases, the discontinuity at ϕ_c decreases and the transition becomes asymptotically continuous, where G is approximately proportional to $\phi - \phi_c$.

Here, we propose a new scaling law for the storage modulus near the transition point:

$$G(\gamma_0, \mu, \phi) = G^{(\text{lin})}(\mu, \phi) \mathcal{F} \left(\frac{\gamma_0}{\mu^{b_1} \{\phi - \phi_c(\mu)\}^{b_2}} \right), \quad (3)$$

where $\mathcal{F}(x)$ is the scaling function satisfying

$$\lim_{x \rightarrow 0} \mathcal{F}(x) = 1, \quad \lim_{x \rightarrow \infty} \mathcal{F}(x) \sim x^{-c} \quad (4)$$

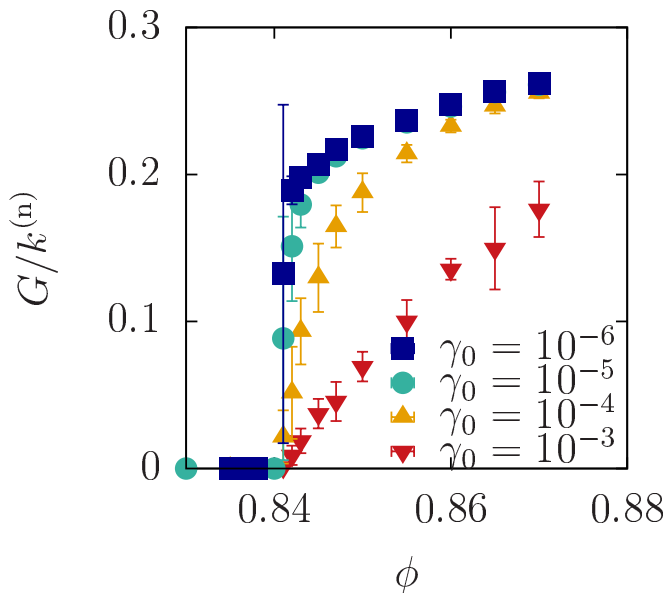


FIG. 3: (Color online) The storage modulus G against ϕ for $\gamma_0 = 10^{-6}, 10^{-5}, 10^{-4}$, and 10^{-3} at $\mu = 0.01$.

with exponents b_1 , b_2 , and c , and we have introduced

$$G^{(\text{lin})}(\mu, \phi) \equiv \lim_{\gamma_0 \rightarrow +0} G(\gamma_0, \mu, \phi). \quad (5)$$

In Eq. (3), we have used the jamming point $\phi_c(\mu)$ depending on μ [56]. Figure 4 confirms the validity of the scaling plot characterized by Eq. (3), where we have determined $G^{(\text{lin})}(\mu, \phi)$ by the extrapolation of the limit $\gamma_0 \rightarrow +0$ using the data for $\gamma_0 \geq 10^{-7}$. The critical exponents used in Eq. (3), are given by [56]

$$b_1 = 1.00 \pm 0.02, \quad b_2 = 0.90 \pm 0.02, \quad c = 1.13 \pm 0.02. \quad (6)$$

It should be noted that the scaling law cannot be applied to the region of the second plateau in Fig. 1

In Eq. (3), we have assumed that the critical strain γ_c characterizing the crossover from the linear to the nonlinear response regimes is proportional to $\mu^{b_1}(\phi - \phi_c)^{b_2}$. The exponents b_1 and b_2 in Eq. (6) may be understood as follows. First, γ_c is expected to satisfy $\gamma_c \sim \delta_c^{(t)}$ with the critical tangential displacement $\delta_c^{(t)}$ characterizing the change of the tangential friction $F^{(t)}$ to the “slip region”. Then, we deduce $\delta_c^{(t)} \sim \mu F^{(n)}$ with the average contact force $F^{(n)} \sim (\phi - \phi_c)$ for grains with the harmonic repulsive interaction [10, 11]. Thanks to the above relations, we obtain $\gamma_c \sim \mu^{b_1}(\phi - \phi_c)^{b_2}$ with $b_1 = 1$ and $b_2 = 1$, which are not far away from the estimated values in Eq. (6). We, however, do not identify the reason why the evaluation of b_2 deviates a little from the numerical value.

It should be noted that the scaling form of Eq. (3) is analogous to that for frictionless case proposed in Ref. [30], though the μ -dependence is not included and c is $1/2$ in the conventional scaling. The main difference between Eq. (3) and the conventional one is that Eq. (3)

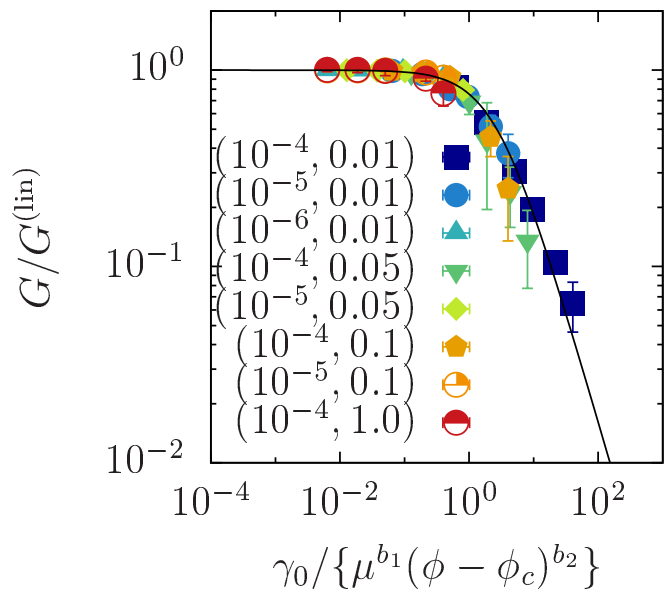


FIG. 4: (Color online) Scaling plot of G characterized by Eq. (3). Each symbol in the legend is characterized by (γ_0, μ) , but each one has the data for $\phi - \phi_c = 0.0001, 0.0002, 0.0005, 0.001$, and 0.01 . The solid line represents the scaling function (S16) in Ref. [56].

represents the crossover from the stick to the slip branch, while the previous scaling deals with the crossover from the slip to the avalanche branch.

We have also confirmed that the storage modulus $G^{(\text{lin})}(\mu, \phi)$ in the linear response regime exhibits a discontinuous transition at ϕ_c . To give further evidence, we plot the storage modulus at ϕ_c defined as

$$G_0(\mu) \equiv \lim_{\phi \rightarrow +\phi_c} G^{(\text{lin})}(\mu, \phi) \quad (7)$$

against μ in Fig. 5, where $G_0(\mu)$ has a maximum value in the frictionless limit. We have also found that $G^{(\text{lin})}(\mu, \phi)$ satisfies

$$G^{(\text{lin})}(\mu, \phi) - G_0(\mu) \propto \{\phi - \phi_c(\mu)\}^a \quad (8)$$

with an exponent $a = 0.52 \pm 0.01$. It should be noted that the previous numerical results suggest $a = 1/2$ [53, 56].

We have summarized our results by two scaling laws derived from Eqs. (3) and (8):

$$\lim_{\gamma_0 \rightarrow +0} G(\gamma_0, \mu, \phi) = G_0(\mu) + A(\mu)\{\phi - \phi_c(\mu)\}^a \quad (9)$$

for the discontinuous transition in the linear response regime and

$$\lim_{\phi \rightarrow +\phi_c} G(\gamma_0, \mu, \phi) \propto G_0(\mu) \left(\frac{\mu^{b_1}(\phi - \phi_c(\mu))^{b_2}}{\gamma_0} \right)^c \quad (10)$$

for the continuous transition in the nonlinear response regime, where $A(\mu)$ depends only on μ . We note that the scaling law, Eq. (10), with $b_2 = 0.90$ and $c \simeq 1.13$

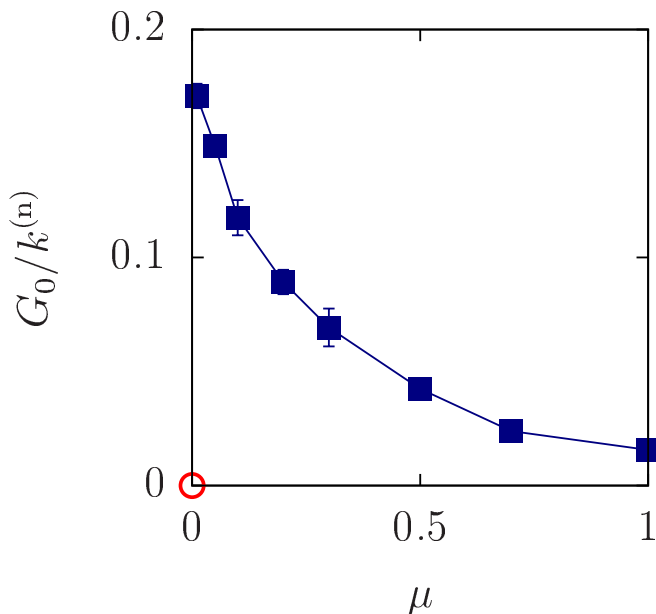


FIG. 5: (Color online) The storage modulus $G_0(\mu)$ for $\mu > 0$ at ϕ_c in the linear response region. The smallest value of μ in this plot is 0.01. The open circle at the origin represents the result for frictionless grains.

indicates $G \sim (\phi - \phi_c)^{b_2c} \simeq (\phi - \phi_c)$ in the nonlinear response regime. This might suggest that the scaling of G is identical to that of the pressure P [30].

Discussion.— Let us discuss our results. Tighe reported that the complex shear modulus G^* for a model of emulsions satisfies $G^* \sim \omega^{1/2}$ near ϕ_c in the linear response regime [61]. On the contrary, we have confirmed that the storage modulus is independent of ω , and the loss modulus is proportional to ω in the linear response regime for all of the packing fractions [56]. It should be noted that the static contact friction and the inertia of the particles exist in our system, but they are not involved in Ref. [61], which might lead to the different dependence of G^* .

In this Letter, we have proposed the scaling law for the shear modulus of grains with the harmonic repulsive interaction. From the analogy of the frictionless case [30], we expect the exponent $b_2 = 3/2$ for Hertzian contact model because of the relation $\gamma_c \sim \delta_c^{(t)} \sim \mu F^{(n)}$ with $F^{(n)} \sim (\phi - \phi_c)^{3/2}$. The confirmation of this conjecture will be the subject of further study.

There are some studies to focus on the role of perco-

lation to the jamming [62–65]. In the system exhibiting a conventional percolation, the critical exponents for the storage modulus depends on the spatial dimension [66], but the exponents of the jamming transition are independent of the dimensionality, at least, for frictionless grains [11]. Further careful study on the relation between percolation and jamming should be necessary.

An important finding of this Letter is the scaling law (3) interpolating between the linear and the nonlinear response regimes for frictional grains. Somfai et al. found that the elastic moduli of frictional grains in the linear response regime is proportional to the excess coordination number ΔZ [53]. Based on this result, a recent review paper suggested that there is no scaling of the mechanical properties as a function of $\phi - \phi_c$ for frictional grains because ΔZ of the frictional grains remains finite even at ϕ_c [2]. Our scaling plot based on Eq. (3), however, gives a counter evidence of the existence of the scaling law. We also note that Ref. [53] have ignored the change of the tangential contact force to the “slip region”, but this effect becomes significant in the vicinity of ϕ_c for finite γ_0 as can be seen in Eq. (3). To our knowledge, this effect has not been indicated in previous studies.

Concluding remarks.— We have numerically investigated the frictional granular particles. The storage modulus in the linear response regime for frictional grains differs from that for frictionless grains even in the zero friction limit, whereas they are almost identical in the nonlinear response regime. This dependence on the tangential friction has been explained from the stress-strain curve shown in Fig. 2. We have also proposed the new scaling law that interpolates between the discontinuous transition for infinitesimal strain and the continuous one for finite strain. This scaling law has been verified through our simulation.

The authors thank O. Dauchot, H. Yoshino, T. Yamaguchi, F. van Wijland, and K. Miyazaki for fruitful discussions. This work is partially supported by the Grant-in-Aid of MEXT for Scientific Research (Grant No. 16H04025 and No. 25800220). One of the authors (M.O.) appreciates the warm hospitality of Yukawa Institute for Theoretical Physics at Kyoto University and the discussions during the YITP workshops “New Frontiers in Non-equilibrium Physics 2015” and “Avalanches, plasticity, and nonlinear response in nonequilibrium”, which helped to complete this work.

[1] A. J. Liu and S. R. Nagel, *Nature* **396**, 21 (1998).
 [2] M. van Hecke, *J. Phys.: Condens. Matter* **22**, 033101 (2009)
 [3] C. S. O’Hern, S. A. Langer, A. J. Liu, and S. R. Nagel, *Phys. Rev. Lett.* **88**, 075507 (2002).
 [4] C. S. O’Hern, L. E. Silbert, A. J. Liu, and S. R. Nagel, *Phys. Rev. E* **68**, 011306 (2003).

[5] P. Olsson and S. Teitel, *Phys. Rev. Lett.* **99**, 178001 (2007).
 [6] T. Hatano, M. Otsuki, and S. Sasa, *J. Phys. Soc. Jpn.* **76**, 023001 (2007).
 [7] T. Hatano, *J. Phys. Soc. Jpn.* **77**, 123002 (2008).
 [8] B. P. Tighe, E. Woldhuis, J. J. C. Remmers, W. van Saarloos, and M. van Hecke, *Phys. Rev. Lett.* **105**, 088303

- (2010).
- [9] T. Hatano, Prog. Theor. Phys. Suppl. **184**, 143 (2010).
- [10] M. Otsuki and H. Hayakawa, Prog. Theor. Phys. **121**, 647 (2009).
- [11] M. Otsuki and H. Hayakawa, Phys. Rev. E **80**, 011308 (2009).
- [12] M. Otsuki, H. Hayakawa, and S. Luding, Prog. Theor. Phys. Suppl. **184**, 110 (2010).
- [13] K. N. Nordstrom, E. Verneuil, P. E. Arratia, A. Basu, Z. Zhang, A. G. Yodh, J. P. Gollub, and D. J. Durian, Phys. Rev. Lett. **105**, 175701 (2010).
- [14] P. Olsson and S. Teitel, Phys. Rev. E **83**, 030302(R) (2011).
- [15] D. Vågberg, P. Olsson, and S. Teitel, Phys. Rev. E **83**, 031307 (2011).
- [16] M. Otsuki and H. Hayakawa, Prog. Theor. Phys. Suppl. **195**, 129 (2012).
- [17] A. Ikeda, L. Berthier, and P. Sollich, Phys. Rev. Lett. **109**, 018301 (2012).
- [18] P. Olsson and S. Teitel, Phys. Rev. Lett. **109**, 108001 (2012).
- [19] E. DeGiuli, G. Düring, E. Lerner, and M. Wyart, Phys. Rev. E **91**, 062206 (2015).
- [20] D. Vågberg, P. Olsson, and S. Teitel Phys. Rev. E **93**, 052902 (2016).
- [21] F. Boyer, E. Guazzelli, and O. Pouliquen, Phys. Rev. Lett. **107**, 188301 (2011).
- [22] M. Trulsson, B. Andreotti, and P. Claudin, Phys. Rev. Lett. **109**, 118305 (2012).
- [23] B. Andreotti, J.-L. Barrat, and C. Heussinger, Phys. Rev. Lett. **109**, 105901 (2012).
- [24] E. Lerner, G. Düring, and M. Wyart, Proc. Natl. Acad. Sci. U.S.A **109**, 4798 (2012).
- [25] D. Vågberg, P. Olsson, and S. Teitel Phys. Rev. Lett. **113**, 148002 (2014).
- [26] T. Kawasaki, D. Coslovich, A. Ikeda, and L. Berthier, Phys. Rev. E **91**, 012203 (2015).
- [27] K. Suzuki and H. Hayakawa, Phys. Rev. Lett. **115**, 098001 (2015).
- [28] M. Wyart, Annales de Physique **30**, 3 (2005).
- [29] C. Coulais, A. Seguin, and O. Dauchot, Phys. Rev. Lett. **113**, 198001 (2014).
- [30] M. Otsuki and H. Hayakawa, Phys. Rev. E **90**, 042202 (2014).
- [31] M. S. van Deen, J. Simon, Z. Zeravcic, S. Dagois-Bohy, B. P. Tighe, and M. van Hecke, Phys. Rev. E **90**, 020202(R) (2014).
- [32] C. P. Goodrich, A. J. Liu, and J. P. Sethna, Proc. Natl. Acad. Sci. USA. **113** 9745 (2016).
- [33] D. Nakayama, H. Yoshino, and F. Zamponi, J. Stat. Mech. 104001 (2016).
- [34] J. Boschan, D. Vagberg, E. Somfai, B. P. Tighe, Soft Matter **12**, 5450 (2016).
- [35] K. Dahmen, D. Ertas, and Y. Ben-Zion, Phys. Rev. E **58**, 1494 (1998).
- [36] K. Dahmen, Y. Ben-Zion, and J. T. Uhl, Nat. Phys. **7**, 554 (2011).
- [37] M. Otsuki and H. Hayakawa, Phys. Rev. E **83**, 051301 (2011).
- [38] D. Bi, J. Zhang, B. Chakraborty and R. Behringer, Nature **480**, 355 (2011).
- [39] S. Chialvo, J. Sun, and S. Sundaresan, Phys. Rev. E **85**, 021305 (2012).
- [40] E. Brown and H. M. Jaeger, Phys. Rev. Lett. **103**, 086001 (2009).
- [41] R. Seto, R. Mari, J. F. Morris, and M. M. Denn, Phys. Rev. Lett. **111**, 218301 (2013).
- [42] N. Fernandez, R. Mani, D. Rinaldi, D. Kadau, M. Mosquet, H. Lombois-Burger, J. Cayer-Barrioz, H. J. Herrmann, N. D. Spencer, and L. Isa, Phys. Rev. Lett. **111**, 108301 (2013).
- [43] C. Heussinger, Phys. Rev. E **88**, 050201 (2013).
- [44] M. M. Bandi, M. K. Rivera, F. Krzakala and R.E. Ecke, Phys. Rev. E **87**, 042205 (2013).
- [45] M. P. Ciamarra, R. Pastore, M. Nicodemi, and A. Coniglio, Phys. Rev. E **84**, 041308 (2011).
- [46] R. Mari, R. Seto, J. F. Morris, and M. M. Denn, J. Rheol. **58**, 1693 (2014).
- [47] M. Grob, C. Heussinger, and A. Zippelius, Phys. Rev. E **89**, 050201 (2014).
- [48] T. Kawasaki, A. Ikeda, and L. Berthier, EPL **107**, 28009 (2014).
- [49] M. Wyart and M. E. Cates, Phys. Rev. Lett. **112**, 098302 (2014).
- [50] M. Grob, A. Zippelius, and C. Heussinger, Phys. Rev. E **93**, 030901 (2016).
- [51] V. Magnanimo, L. La Ragione, J. T. Jenkins, P. Wang, and H. A. Makse, EPL **81**, 34006 (2008).
- [52] H. Hayakawa and S. Takada, arXiv:1611.07925.
- [53] E. Somfai, M. van Hecke, W. G. Ellenbroek, K. Shundyak, and W. van Saarloos, Phys. Rev. E **75**, 020301(R) (2007).
- [54] P. Cundall and O. D. L. Strack, Geotechnique **29**, 47 (1979).
- [55] M. Doi and S. F. Edwards, *The Theory of Polymer Dynamics* (Oxford University Press, Oxford, 1990).
- [56] See Supplemental Material, which includes Ref. [57–60], for the details of the analysis and supplementary simulation results.
- [57] D. J. Evans and G. P. Morriss, *Statistical Mechanics of Nonequilibrium Liquids* 2nd ed. (Cambridge University Press, Cambridge, 2008).
- [58] W. H. Press, S. A. Teukolsky, W. T. Vetterling, and B. P. Flannery, *Numerical Recipes*, 3rd ed. (Cambridge University Press, Cambridge, 2007).
- [59] L. E. Silbert, Soft Matter **6**, 2918 (2010)
- [60] L. E. Silbert, D. Ertas, G. S. Grest, T. C. Halsey, and D. Levine, Phys. Rev. E **65**, 031304 (2002).
- [61] B. P. Tighe, Phys. Rev. Lett. **107**, 158303 (2011).
- [62] G. Lois, J. Blawdziewicz, and C. S. O'Hern, Phys. Rev. Lett. **100**, 028001 (2008).
- [63] T. Shen, C. S. O'Hern, M. D. Shattuck, Phys. Rev. E **85**, 011308 (2012).
- [64] L. Kovaleva, A. Goulet, and L. Kondic, Phys. Rev. E **92**, 032204 (2015).
- [65] S. Henkes, D. A. Quint, Y. Fily, and J. M. Schwarz, Phys. Rev. Lett. **116**, 028301 (2016).
- [66] S. Torquato, *Random Heterogeneous Materials: Microstructure and Macroscopic Properties*, 2nd ed. (Springer, New York, 2005).

Supplemental Materials: **

I. INTRODUCTION

In this Supplemental Materials, we present details and additional results of our model. We explain the setup of our simulation in Sec. II. In Sec. III, we demonstrate the dependence of the complex shear modulus on the angular frequency ω . Section IV deals with the stress-strain curves for various γ_0 . In Sec. V, we explain the method to determine the exponents for the scaling law proposed in the main text. We present the method to determine the transition point depending on the friction coefficient μ in Sec. VI. In Sec. VII, we show numerical results for the storage modulus in the linear response regime.

II. DETAILS OF OUR SIMULATION

In this section, we explain our setup and model. The position, the velocity, and the angular velocity of the grain i are, respectively, denoted by \mathbf{r}_i , \mathbf{v}_i , and $\omega_i \hat{\mathbf{z}}$, where we have introduced the unit vector $\hat{\mathbf{z}}$ parallel to z axis (perpendicular to the considering plane). The contact force \mathbf{F}_{ij} between the grain i and the grain j consists of the normal part $\mathbf{F}_{ij}^{(n)}$ and the tangential part $\mathbf{F}_{ij}^{(t)}$ as $\mathbf{F}_{ij} = \mathbf{F}_{ij}^{(n)} + \mathbf{F}_{ij}^{(t)}$. The normal contact force $\mathbf{F}_{ij}^{(n)}$ is given by

$$\mathbf{F}_{ij}^{(n)} = \mathbf{F}_{ij}^{(n,\text{el})} + \mathbf{F}_{ij}^{(n,\text{vis})}, \quad (\text{S1})$$

where

$$\mathbf{F}_{ij}^{(n,\text{el})} = k^{(n)}(d_{ij} - |\mathbf{r}_{ij}|)\Theta(d_{ij} - |\mathbf{r}_{ij}|)\mathbf{n}_{ij}, \quad (\text{S2})$$

$$\mathbf{F}_{ij}^{(n,\text{vis})} = -\eta^{(n)}v_{ij}^{(n)}\Theta(d_{ij} - |\mathbf{r}_{ij}|)\mathbf{n}_{ij} \quad (\text{S3})$$

with the normal spring constant $k^{(n)}$ and the normal viscous constant $\eta^{(n)}$. Here, \mathbf{r}_{ij} , \mathbf{n}_{ij} , $v_{ij}^{(n)}$, and d_{ij} are, respectively, given by $\mathbf{r}_{ij} = \mathbf{r}_i - \mathbf{r}_j$, $\mathbf{n}_{ij} = \mathbf{r}_{ij}/|\mathbf{r}_{ij}|$, $v_{ij}^{(n)} = (\mathbf{v}_i - \mathbf{v}_j) \cdot \mathbf{n}_{ij}$, and $d_{ij} = (d_i + d_j)/2$ with the diameter d_i of the grain i . In Eqs. (S2) and (S3), we have introduced the Heaviside step function $\Theta(x)$ defined by $\Theta(x) = 1$ for $x \geq 0$ and $\Theta(x) = 0$ otherwise.

Similarly, the tangential friction force $\mathbf{F}_{ij}^{(t)}$ is given by

$$\mathbf{F}_{ij}^{(t)} = \min\left(\tilde{F}_{ij}^{(t)}, \mu|\mathbf{F}_{ij}^{(n,\text{el})}|\right) \text{sign}\left(\tilde{F}_{ij}^{(t)}\right) \mathbf{t}_{ij}, \quad (\text{S4})$$

where $\min(a, b)$ selects the smaller one between a and b , $\text{sign}(x)$ is 1 for $x > 0$ and -1 for $x < 0$, and $\tilde{F}_{ij}^{(t)}$ is given by

$$\tilde{F}_{ij}^{(t)} = k^{(t)}\delta_{ij}^{(t)} - \eta^{(t)}v_{ij}^{(t)} \quad (\text{S5})$$

with $\mathbf{t}_{ij} = (-r_{ij,y}/|\mathbf{r}_{ij}|, r_{ij,x}/|\mathbf{r}_{ij}|)$. Here, $k^{(t)}$, $\eta^{(t)}$, and μ are the tangential spring constant, the tangential viscous constant, and the friction coefficient, respectively. The tangential velocity $v_{ij}^{(t)}$ and the tangential displacement $\delta_{ij}^{(t)}$ are, respectively, given by

$$v_{ij}^{(t)} = (\mathbf{v}_i - \mathbf{v}_j) \cdot \mathbf{t}_{ij} - (d_i\omega_i + d_j\omega_j)/2, \quad (\text{S6})$$

$$\delta_{ij}^{(t)} = \int_{\text{stick}} dt v_{ij}^{(t)}, \quad (\text{S7})$$

where ‘‘stick’’ on the integral implies that the integral is only performed when the condition $|\tilde{F}_{ij}^{(t)}| < \mu|\mathbf{F}_{ij}^{(n,\text{el})}|$ is satisfied. Additionally, we have introduced the torque T_i on the grain i as

$$T_i = -\sum_j \frac{d_j}{2} \mathbf{F}_{ij}^{(t)} \cdot \mathbf{t}_{ij}. \quad (\text{S8})$$

In this model, we apply an oscillatory shear along the y direction under the Lees-Edwards boundary condition [S1]. The SLLOD equations of motion are used to stabilize the uniform sheared state as

$$\frac{d\mathbf{r}_i}{dt} = \frac{\mathbf{p}_i}{m_i} + \dot{\gamma}(t)r_{i,y}\hat{\mathbf{x}}, \quad (\text{S9})$$

$$\frac{d\mathbf{p}_i}{dt} = \sum_{j \neq i} \mathbf{F}_{ij} - \dot{\gamma}(t)p_{i,y}\hat{\mathbf{x}}, \quad (\text{S10})$$

$$I_i \frac{d\omega_i}{dt} = T_i, \quad (\text{S11})$$

where we have introduced the time dependent shear rate $\dot{\gamma}(t)$, the peculiar momentum \mathbf{p}_i defined by Eq. (S9), the unit vector parallel to the x -direction $\hat{\mathbf{x}}$, the mass $m_i = \pi\rho d_i^2/4$, and the moment of inertia $I_i = m_i d_i^2/8$.

As an initial state, the disks are randomly placed in the system with the initial packing fraction $\phi_I = 0.75$. After relaxing the system to a mechanical equilibrium state, we compress the system without shear in small steps until the packing fraction reaches a given value ϕ . In each step, we change the linear system size and the position of the grain i as

$$L^{(n_s+1)} = L^{(n_s)} \sqrt{\frac{\phi^{(n_s)}}{\phi^{(n_s+1)}}}, \quad (\text{S12})$$

$$\mathbf{r}_i^{(n_s+1)} = \mathbf{r}_i^{(n_s)} \sqrt{\frac{\phi^{(n_s)}}{\phi^{(n_s+1)}}}, \quad (\text{S13})$$

and relax the grains to the mechanical equilibrium state. Here, $L^{(n_s)}$, $\mathbf{r}_i^{(n_s)}$, and $\phi^{(n_s)}$ denote the system size, the position of the grains i , and the packing fraction at the n_s -th step, respectively. The increment of the packing fraction is defined by $\Delta\phi \equiv \phi^{(n_s+1)} - \phi^{(n_s)}$. Here, we regard the state for $T < T_{\text{th}}$ as the mechanical equilibrium state, where we have introduced the kinetic temperature $T \equiv \sum_i |\mathbf{p}_i|^2 / (2m_i N)$ and a threshold T_{th} . It should be

noted that the origin of the coordinate axes is located at the center of the system.

Let us summarize a set of parameters used in our simulation. We use $k^{(t)} = k^{(n)}$ and $\eta^{(n)} = \eta^{(t)} = \sqrt{m_0 k^{(n)}}$, where m_0 is the mass of a grain with the diameter d_0 . This set of the parameters corresponds to the constant restitution coefficient $e = 0.043$. We adopt the leapfrog algorithm with the time step $\Delta t = 0.05\tau$, where τ is the characteristic time of the stiffness, i.e., $\tau = \sqrt{m_0/k^{(n)}}$. The number N of the grains is 4000. We have checked that the shear modulus is independent of N for $N \geq 4000$. We fix the parameters $T_{\text{th}} = 10^{-8}(k^{(n)}d_0^2)$, $\Delta\phi = 10^{-4}$, and $\omega = 10^{-4}\tau^{-1}$ in the main text, but we have examined the ω -dependence of the complex modulus in the next section. We have confirmed that our results in the main text are insensitive to T_{th} , $\Delta\phi$ and ω if they are sufficiently small. Here, the storage modulus G is calculated from Eq. (1) in the main text with the aid of the shear stress $\sigma(t)$ given by

$$\begin{aligned} \sigma(t) = & -\frac{1}{L^2} \sum_i^N \sum_{j>i} r_{ij,x}(t) F_{ij,y}(t) \\ & -\frac{1}{L^2} \sum_i^N \frac{p_{i,x}(t)p_{i,y}(t)}{m_i}. \end{aligned} \quad (\text{S14})$$

III. FREQUENCY DEPENDENCE OF STORAGE AND LOSS MODULI

This section deals with the dependence of the complex shear modulus $G^* = G + iG''$ on ω in the linear response regime. In Fig. S1, we show the storage modulus G against ω for various ϕ at $\mu = 1.0$ and $\gamma_0 = 10^{-7}$. As shown in Fig. S1, G for each ϕ is almost independent of ω for $\omega\tau < 10^{-2}$. Hence, we have not discussed the ω -dependence of G in the main text.

Figure S2 exhibits the loss modulus G'' against ω for various ϕ at $\mu = 1.0$ and $\gamma_0 = 10^{-7}$. Here, G'' is given by

$$G'' = \frac{\omega}{\pi} \int_0^{2\pi/\omega} dt \sigma(t) \sin(\omega t) / \gamma_0. \quad (\text{S15})$$

As shown in Fig. S2, G'' is almost proportional to ω . These ω dependences of G and G'' indicate that the rheological properties in our model are essentially described by the Kelvin-Voigt viscoelasticity. This result is reasonable because the Cundall-Strack model relies on the Kelvin-Voigt model [S2]. Moreover, the ϕ -dependence of G'' is not clearly visible. Hence, we have investigated only G in the main text.

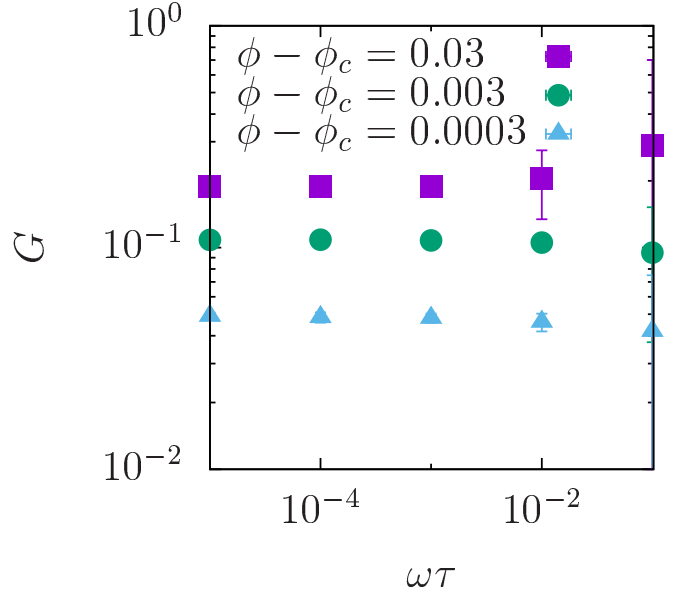


FIG. S1: The storage modulus G against ω for $\phi - \phi_c = 0.03, 0.003$ and 0.0003 at $\mu = 1.0$ and $\gamma_0 = 10^{-7}$.

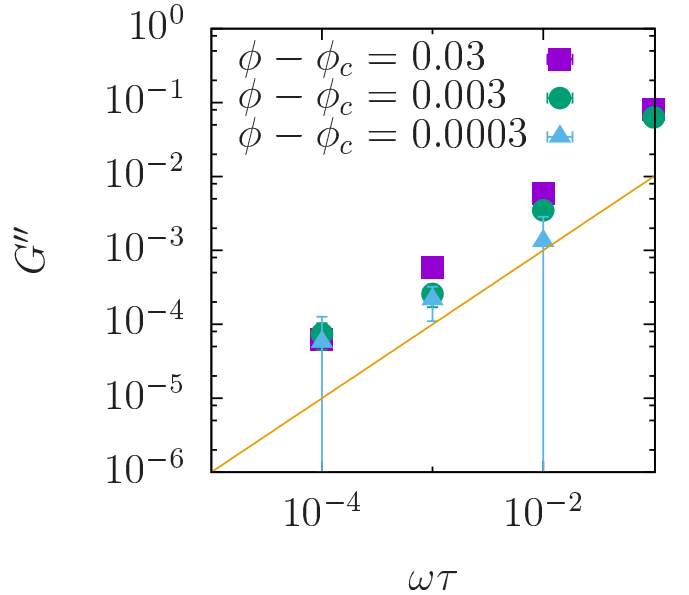


FIG. S2: The loss modulus G'' against ω for $\phi - \phi_c = 0.03, 0.003$ and 0.0003 at $\mu = 1.0$ and $\gamma_0 = 10^{-7}$. The solid line represents $G'' \sim \omega$.

IV. THE STRESS-STRAIN CURVES FOR VARIOUS γ_0

In this section, we demonstrate the dependence of the stress-strain curve on γ_0 . Figure S3 exhibits the intrinsic shear stress $\sigma(\gamma) - \sigma(0)$ against the shear strain γ for various γ_0 at $\mu = 10^{-6}$ and $\phi = 0.87$. For $\gamma_0 = 10^{-7}$, $\sigma(\gamma) - \sigma(0)$ is proportional to γ , but the constant of proportionality is larger than that of frictionless grains indicated by the dotted line. The reason for the difference

in the constant of proportionality is that the increase of the tangential friction force $|\mathbf{F}_{ij}^{(t)}|$ in the “stick region” enlarges $\sigma(\gamma) - \sigma(0)$ for $\mu > 0$ under sufficiently small γ . As γ_0 increases, the stress-strain curve exhibits a nonlinear behavior: a hysteresis loop to connect the first linear region for sufficiently small γ with the second linear region for $\gamma > 10^{-6}$, where the gradient of the second linear region is identical to that of the frictionless grains. The second linear region originates from the fact that $|\mathbf{F}_{ij}^{(t)}|$ remains constant in the “slip region” and does not contribute to enlarge $\sigma(\gamma) - \sigma(0)$.

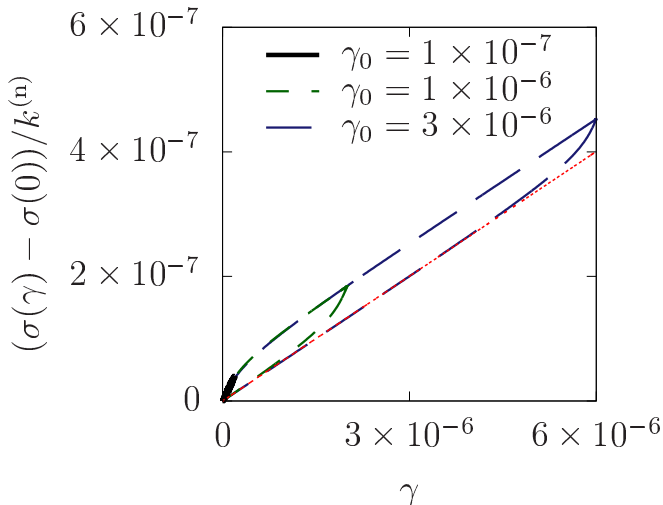


FIG. S3: The intrinsic shear stress $\sigma(\gamma) - \sigma(0)$ against γ for $\gamma_0 = 3.0 \times 10^{-6}$, 1.0×10^{-6} , and 1.0×10^{-7} at $\mu = 10^{-6}$ and $\phi = 0.87$. The dotted line indicates $\sigma(\gamma) - \sigma(0)$ for $\gamma_0 = 3.0 \times 10^{-6}$ at $\mu = 0$ and $\phi = 0.87$.

V. METHOD TO DETERMINE THE EXPONENTS

In this section, we explain the method to determine the exponents in the scaling plot proposed in the main text. Here, the exponents are determined by Levenberg-Marquardt algorithm [S3], where we have assumed the functional form of the scaling function as

$$\mathcal{F}(x) = \frac{1}{1 + e^{\sum_{n=0}^{N_n} A_n (\ln x)^n}} \quad (\text{S16})$$

with the fitting parameters $N_n = 1$, $A_0 = -1.13 \pm 0.22$, and $A_1 = 1.13 \pm 0.02$. We have checked the numerical estimation of b_1 and b_2 with $N_n \geq 2$, but A_n for $n \geq 2$ are almost 0, implying that the exponent c in Eq. (4) of the main text is approximately equal to $c \approx A_1 = 1.13$.

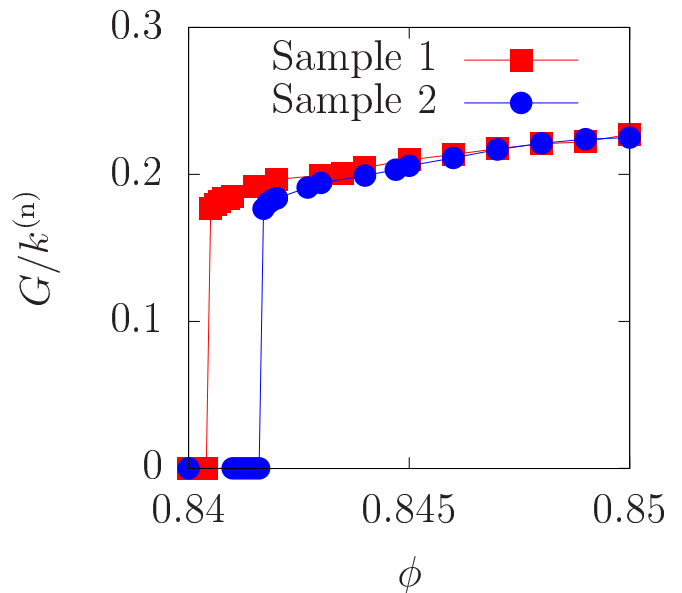


FIG. S4: The storage modulus G against ϕ at $\mu = 0.01$ and $\gamma_0 = 10^{-7}$. “Sample 1” and “Sample 2” indicate the data obtained from different initial configurations, respectively.

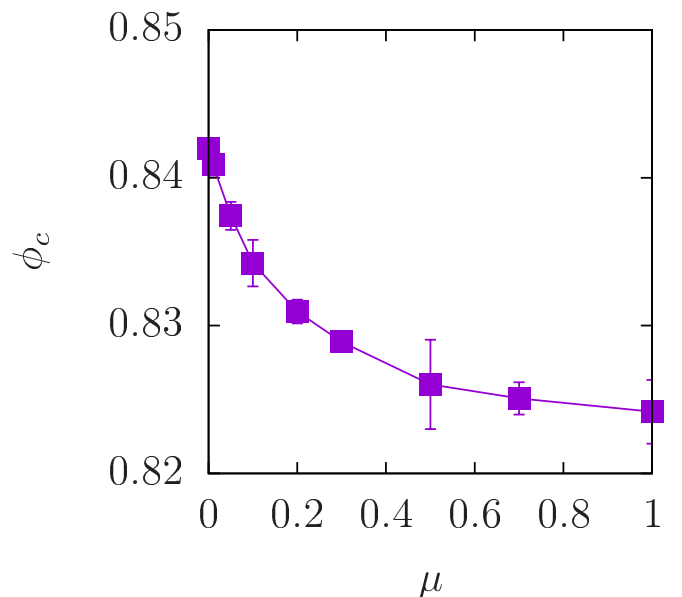


FIG. S5: The plots of transition points ϕ_c against μ .

VI. DETERMINATION OF TRANSITION POINT

In this section, we explain the method to determine the transition point $\phi_c(\mu)$. To estimate $\phi_c(\mu)$, we first prepare assemblies with different packing fractions obtained from the same initial configuration of grains with the friction coefficient μ . Then, we apply the oscillatory shear to measure G for sufficiently small shear amplitude ($\gamma_0 = 10^{-7}$), and plot G against ϕ as shown in Fig. S4, which plots the data at $\mu = 0.01$ and $\gamma_0 = 10^{-7}$ ob-

tained from different initial configurations. G changes discontinuously around $\phi = 0.84$, but the critical fraction depends on the initial configuration. Then, we define $\phi_c(\mu)$ for each initial configuration as the minimum value of ϕ where G for a given initial configuration exceeds $G_{\text{th}} = 10^{-3}k^{(n)}$. In Fig. S5, we plot the average of $\phi_c(\mu)$ against μ . $\phi_c(\mu)$ decreases with increasing μ , which is consistent with the previous numerical results [S4, S5].

VII. THE STORAGE MODULUS IN THE LINEAR RESPONSE REGIME

In this section, we investigate the storage modulus in the linear response regime. Figure S6 plots $G_0(\mu)$ against the the excess coordination number $Z_0(\mu) - Z_{\text{iso}}$ for various μ , where $Z_0(\mu)$ and $Z_{\text{iso}} = 3$ are the coordination number at ϕ_c and the isostatic value of the coordination number for two dimensional frictional grains, respectively. As shown in Ref. [S6], $G_0(\mu)$ satisfies

$$G_0(\mu) \propto Z_0(\mu) - Z_{\text{iso}}. \quad (\text{S17})$$

It is known that $Z_0(\mu)$ continuously decreases with increasing μ from the isostatic value, 4, for frictionless grains [S4–S7]. $Z_0(\mu)$ in our model exhibits the identical behavior as shown in Fig. S7. It should be noted that $Z_0(\mu)$ in our system under oscillatory shear is qualitatively consistent with that of the previous result under steady shear [S5]. These results explain the decrease of $G_0(\mu)$ with increasing μ shown in Fig. 5 of the main text.

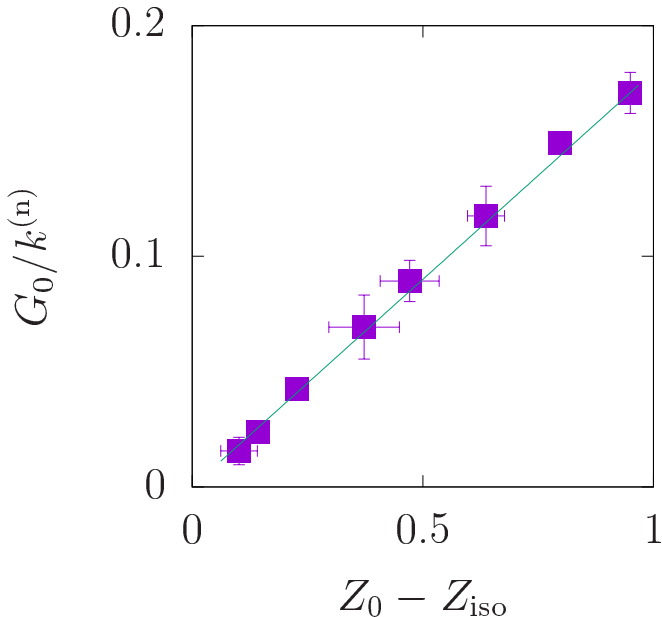


FIG. S6: $G_0(\mu)$ against $Z_0(\mu) - Z_{\text{iso}}$ for $\mu = 0.01, 0.05, 0.1, 0.2, 0.3, 0.5, 0.7$, and 1.0 . The solid line represents Eq. (S17).

We have also found that $G^{(\text{lin})}(\mu, \phi)$ satisfies Eq. (8) in the main text, which is verified in Fig. S8. In the inset

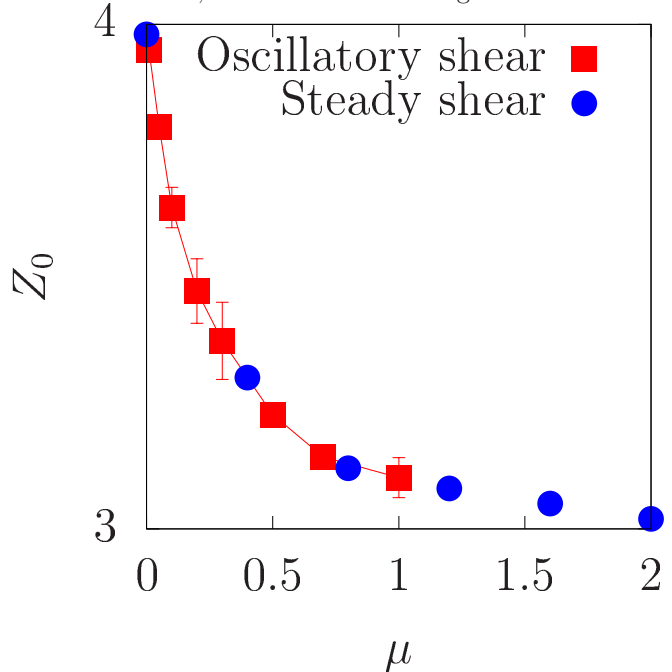


FIG. S7: The coordination number Z_0 at the transition point ϕ_c against μ for the present system under oscillatory shear and the system in Ref. [S5] under steady shear.

of Fig. S8, we plot the exponent a evaluated by the least squares method against μ , which is almost independent of μ and estimated as $a = 0.52 \pm 0.1$.

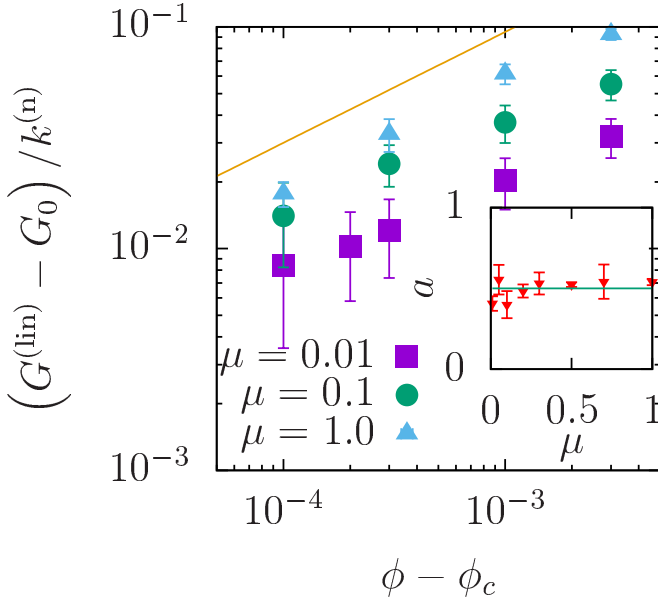


FIG. S8: $G^{(\text{lin})}(\mu, \phi) - G_0(\mu)$ against $\phi - \phi_c(\mu)$ for $\mu = 0.01, 0.05, 0.1, 0.5$, and 1.0 . The solid line represents Eq. (8) in the main text with $a = 1/2$. (Inset) The exponent a evaluated by the least squares method against μ . The solid line represents $a = 1/2$.

[S1] D. J. Evans and G. P. Morriss, *Statistical Mechanics of Nonequilibrium Liquids* 2nd ed. (Cambridge University Press, Cambridge, 2008).
[S2] P. Cundall and O. D. L. Strack, *Geotechnique* **29**, 47 (1979).
[S3] W. H. Press, S. A. Teukolsky, W. T. Vetterling, and B. P. Flannery, *Numerical Recipes*, 3rd ed. (Cambridge University Press, Cambridge, 2007).
[S4] L. E. Silbert, *Soft Matter* **6**, 2918 (2010)

[S5] M. Otsuki and H. Hayakawa, *Phys. Rev. E* **83**, 051301 (2011).
[S6] E. Somfai, M. van Hecke, W. G. Ellenbroek, K. Shundyak, and W. van Saarloos, *Phys. Rev. E* **75**, 020301(R) (2007).
[S7] L. E. Silbert, D. Ertag, G. S. Grest, T. C. Halsey, and D. Levine, *Phys. Rev. E* **65**, 031304 (2002).